Star clusters: basic galactic building blocks
Proceedings IAU Symposium No. 266, 2009
R. de Grijs & J. R. D. Lépine, eds.

doi:10.1017/S1743921309991591

Tracing star cluster formation in the interacting galaxy M51

Narae Hwang[1,2] **and Myung Gyoon Lee**[2]

[1]National Astronomical Observatory of Japan, 2-21-1 Osawa, Mitaka, Tokyo 181-8588, Japan
email: narae.hwang@nao.ac.jp

[2]Department of Physics and Astronomy, Seoul National University, 599 Gwanak-ro, Gwanak-gu, Seoul 151-747, Republic of Korea
email: mglee@astro.snu.ac.kr

Abstract. We present a study of star clusters in the interacting galaxy M51 using a star cluster catalog that includes about 3600 star clusters with $m_{\rm F555W} < 23$ mag, compiled by Hwang & Lee (2008). Combined with $m_{\rm F336W}$-band imaging data taken with the *Hubble Space Telescope (HST)*'s WFPC2 camera, we have derived the ages and masses of star clusters in M51 using theoretical population synthesis models. The cluster age distribution displays multiple peaks that correspond to the epochs of dynamical encounters predicted by theoretical model studies and the cluster-formation rate appears to increase around the same epochs.

Keywords. galaxies: individual (M 51, NGC 5194, NGC 5195), galaxies: star clusters, galaxies: evolution, galaxies: interactions

1. Introduction

Star clusters in M51, an interacting galaxy system composed of the Sbc-type spiral galaxy NGC 5194 and the SB0 galaxy NGC 5195, provide a unique opportunity to understand star cluster formation and evolution in the context of dynamical interactions of their host galaxies. There are some theoretical (Toomre & Toomre 1972; Salo & Laurikainen 2000) and observational (Durrell *et al.* 2003) studies suggesting that the two galaxies may have experienced a single or multiple encounters a few hundred Myr ago. M51 is located at a distance of 8.4 Mpc (Feldmeier *et al.* 1997) so that, with the resolving power of *HST*, it is possible to marginally resolve individual star clusters.

We have carried out star cluster surveys using the deep and wide-field image data of M51 taken with *HST*/ACS and have compiled a catalog of about 3600 star clusters in M51 (Hwang & Lee 2008). The same image data have been used in several studies of M51 star clusters, such as of faint fuzzy clusters (Hwang & Lee 2006), the cluster size distribution (Scheepmaker *et al.* 2007), the cluster luminosity function (Haas *et al.* 2008) and the radial distribution of cluster formation (Scheepmaker *et al.* 2009). We have also analyzed $m_{\rm F336W}$-band image data of M51 taken with *HST*/WFPC2 and have combined the $m_{\rm F336W}$-band photometry with the photometric catalog of Hwang & Lee (2008) to estimate the ages and masses of star clusters. The theoretical population synthesis models of Bruzual & Charlot (2003) were used for age and mass estimation. The total number of star clusters with derived ages and masses is about 2000. For further information, see Hwang & Lee (2009).

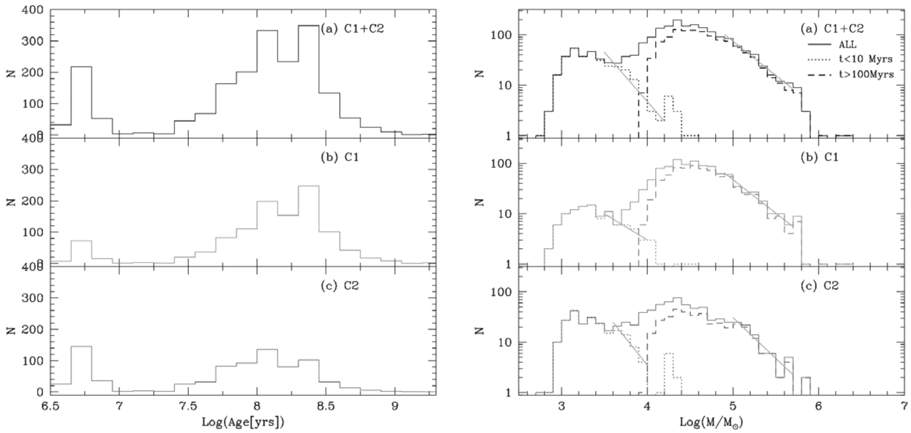

Figure 1. Age *(left)* and mass distribution *(right)* of the M51 Class 1 (C1) and Class 2 (C2) star clusters. There are prominent age peaks at about 100 and 250 Myr. The mass function is exponential and the slope of old component is relatively shallow compared with that of the young component.

2. Age and mass distributions

The age and mass distributions of the M51 star clusters are shown in Figure 1. The age distribution displays two overdense epochs, one at $\log(t/\text{yr}) < 7$ and the other at $7.5 < \log(t/\text{yr}) < 9.0$. The distribution in the latter epoch exhibits two peaks at about 100 and 250 Myr. This is true for both Class 1 (circular shape and isolated) and Class 2 (irregular shape and/or having neighbors) clusters. The large number of clusters with $7.5 < \log(t/\text{yr}) < 9.0$ is consistent with Lee *et al.* (2005), in which the number of star clusters with ages of 100–400 Myr was found to be larger in M51 than in the late-type galaxy M101.

The derived star cluster masses range from 10^3 to 10^6 $M_\odot$ and the mass distribution is composed of two components with different ages. These two components can be represented by a power law with a slope of $\alpha = -2.23 \pm 0.34$ for $t < 10$ Myr and $\alpha = -1.37 \pm 0.11$ for $t > 100$ Myr. The slope of the young cluster mass distribution is in agreement with the initial mass function slope $\alpha \approx -2.0$ of star clusters in late-type galaxies (e.g., Gieles *et al.* 2006).

Figure 2 displays the spatial distribution of star clusters with $\log(t/\text{yr}) < 7$ (young and less massive) and $8.0 < \log(t/\text{yr}) < 8.6$ (intermediate age and more massive) along with the distribution of very luminous HII regions with $L_{\text{H}\alpha} > 10^{37.5}$ erg s^{-1} (J. H. Lee *et al.*, in prep.). It shows a subtle difference in the spatial distribution of young and intermediate-age clusters. Although star clusters are mostly found along the spiral arms of M51, young clusters are preferentially concentrated in the regions where luminous HII regions are found, while intermediate-age clusters are distributed over the entire spiral-arm structure.

3. Star cluster formation rate

We have derived star cluster formation rate using star clusters with $4.6 < \log(M/\text{M}_\odot) < 5.0$ and $\log(M/\text{M}_\odot) > 5.0$. Only star clusters with $m_{\text{F336W}} < 22$ mag were selected for the cluster-formation-rate calculation to reduce the effects of incompleteness which can be very severe for clusters of $\log(t/\text{yr}) > 8.5$. The result is shown in Figure 3, where solid (dashed) lines display the cluster-formation rate derived from the observed (extrapolated

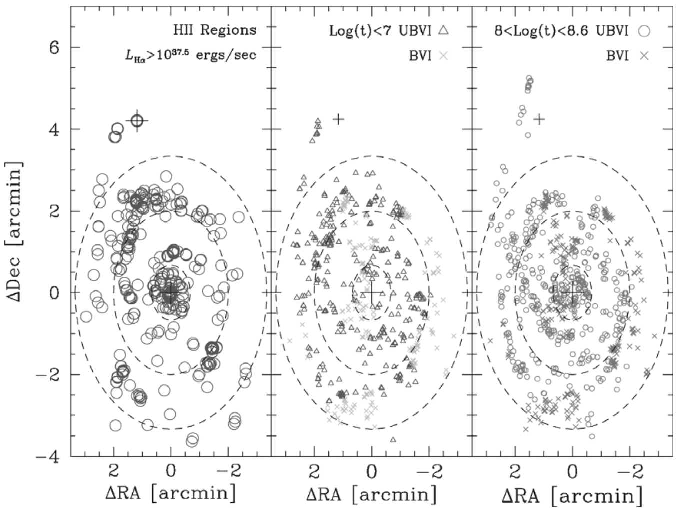

Figure 2. Spatial distribution of HII regions with $L_{\mathrm{H}\alpha} > 10^{37.5}$ erg s^{-1} *(left)* compared with the spatial distribution of the young ($\log(t/\mathrm{yr}) < 7$; *middle*) and intermediate-age ($8 < \log(t/\mathrm{yr}) < 8.6$; *right*) star clusters in M51.

model) cluster age distribution. The extrapolated model age distribution was constructed by fitting the mass distribution of star clusters to a power law and then adding up the derived power-law distribution in the corresponding age bin.

Figure 3 suggests that the cluster-formation rate significantly increased at about 250 Myr and decreased thereafter. This can be seen from star clusters with $4.6 < \log(M/\mathrm{M}_\odot) < 5.0$ and $\log(M/\mathrm{M}_\odot) > 5.0$, respectively. Interestingly, this period is consistent with the theoretically expected interaction epoch of M51 (Toomre & Toomre 1972; Salo & Laurikainen 2000; Durrell *et al.* 2003). Combined with the age distribution which displays a peak at 250 Myr, this result of an enhanced cluster-formation rate during the same period suggests that the dynamical interaction expected to happen around this period may have significantly induced the formation of star clusters.

4. Implication

Dynamical galaxy interactions are believed to have a very strong impact on the formation and disruption of star clusters. However, studies on the dynamical evolution of galaxies and their star cluster populations have been carried out rather independently. With the available theoretical studies on dynamical interactions, M51 provides a unique opportunity for us to compare the evolution of dynamical events and the stellar population in the corresponding galaxies over a certain time interval.

We have shown that the number and the formation rate of star clusters in M51 significantly increased around a certain period. This period is consistent with the theoretically expected epoch of dynamical interactions between NGC 5194 and NGC 5195. However, to fully understand the mechanism and correlation of star cluster formation and galaxy dynamical interaction, we need spectroscopic observations of the star clusters. When we can compare the velocity distribution of star clusters with theoretical models of galaxy interactions, we will be able to understand exactly when and how effectively star clusters are formed and where star clusters are dispersed thereafter. Based on these studies, we

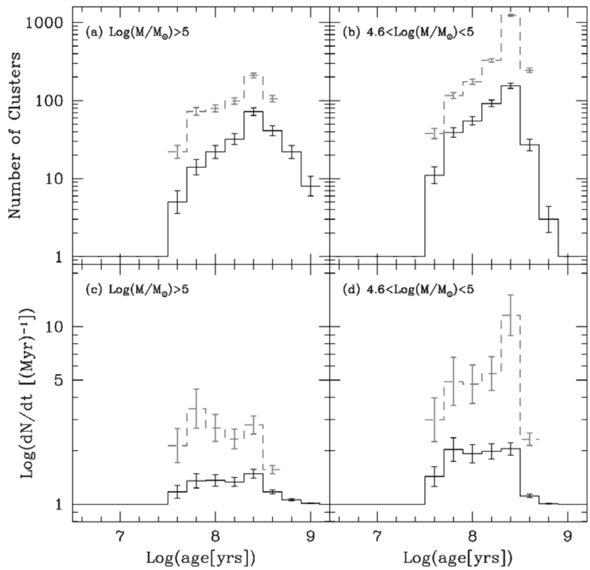

Figure 3. Number distribution and cluster-formation rate for clusters with $\log(M/\mathrm{M}_{\odot}) > 5.0$ *(left)* and $4.6 < \log(M/\mathrm{M}_{\odot}) < 5.0$ *(right)*. The black solid line shows the observed data, while the red dashed line shows the extrapolated data from the best-fit mass function in the corresponding age bins.

would be able to test and improve the existing theoretical models for galaxy interactions that can be applied to other general classes of galaxies.

Acknowledgements

NH acknowledges support from a Grant-in-Aid for JSPS Fellows, No. 20-08325, and travel support from the IAU. MGL is supported in part by a grant (R01-2007-000-20336-0) from the Basic Research Program of the Korea Science and Engineering Foundation.

References

Bruzual, G. & Charlot, S. 2003 *MNRAS*, 344, 1000
Durrell, P. R., Mihos, J. C., Feldmeier, J. J., Jacoby, G. H., & Ciardullo, R. 2002, *ApJ*, 582, 170
Feldmeier, J. J., Ciardullo, R., & Jacoby, G. H. 1997, *ApJ*, 479, 231
Gieles, M., Larsen, S. S., Bastian, N., & Stein, I. T. 2006, *A&A*, 450, 129
Haas, M. R., Gieles, M., Scheepmaker, R. A., Larsen, S. S., & Lamers, H. J. G. L. M. 2008, *A&A*, 487, 937
Hwang, N. & Lee, M. G. 2006, *ApJ* (Letters), 638, L79
Hwang, N. & Lee, M. G. 2008, *AJ*, 135, 1567
Hwang, N. & Lee, M. G. 2009, *ApJ*, in press (arXiv:0912.0321)
Lee, M. G., Chandar, R., & Whitmore, B. W. 2005, *AJ*, 130, 2128
Salo, H. & Laurikainen, E. 2000, *MNRAS*, 319, 377
Scheepmaker, R. A., Haas, M. R., Gieles, M., Bastian, N., Larsen, S. S., & Lamers, H. J. G. L. M. 2007, *A&A*, 469, 925
Scheepmaker, R. A., Lamers, H. J. G. L. M., Lamers, Anders, P., & Larsen, S. S. 2009, *A&A*, 494, 81
Toomre, R. P. J. & Toomre, J. 1972, *ApJ*, 178, 623